

RESEARCH NOTE

Skeletal Ni Catalyst Prepared from a Rapidly Quenched Ni–Al Alloy and Its High Selectivity in 2-Ethylanthraquinone Hydrogenation

Bo Liu,* Minghua Qiao,* Jing-Fa Deng,* Kangnian Fan,* Xiaoxin Zhang,† and Baoning Zong†

*Department of Chemistry, Fudan University, Shanghai 200433, People's Republic of China; and †Research Institute of Petroleum Processing, Beijing 100083, People's Republic of China
E-mail: knfan@fudan.edu.cn

Received March 6, 2001; revised August 31, 2001; accepted August 31, 2001

A novel skeletal Ni catalyst, prepared by alkali leaching of a Ni–Al alloy obtained by the rapid quenching technique, exhibited higher selectivity in hydrogenation of 2-ethylanthraquinone to “active quinones” than that of the Raney Ni catalyst originating from a conventional alloy. It is suggested that the structural defects of the rapidly quenched alloy lead to a high population of the strongly bound hydrogen, which is essential for selective hydrogenation of the carbonyl group. © 2001 Elsevier Science

Key Words: skeletal Ni; rapid quenching; 2-ethylanthraquinone; hydrogenation; hydrogen peroxide.

INTRODUCTION

Hydrogenation of 2-ethylanthraquinone (eAQ) is the key step in the industrial production of H₂O₂ (1–4). As shown in Scheme 1, the hydrogenation products, 2-ethylanthrahydroquinone (eAQH₂) and 2-ethyltetrahydroanthrahydroquinone (H₄eAQH₂), the “active quinones” (5), can be oxidized to produce H₂O₂. Other deep hydrogenation and hydrogenolysis products (degradation products) such as 2-ethylocthydroanthrahydroquinone (H₈eAQH₂), 2-ethylanthracene (eAT), and 2-ethylanthrone (eAN) are not desirable because they can neither produce H₂O₂ nor be regenerated, which leads to the loss of expensive eAQ.

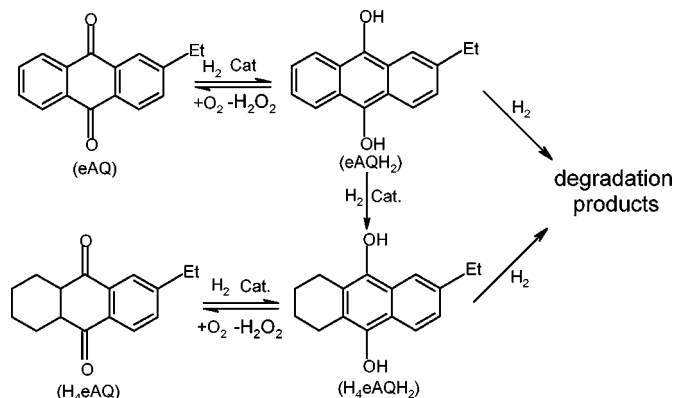
Industrially, the palladium catalysts in the form of palladium black, wire screen, or supported are used in eAQ hydrogenation instead of Raney Ni due to their higher selectivity to “active quinones” (2). However, the cost of the palladium-based catalysts is much higher than that of Raney Ni. In this Research Note, an attempt to develop a kind of novel skeletal Ni catalyst (designated as RQ-Ni) via the rapid quenching technique has been made. When using this catalyst in eAQ hydrogenation, a high yield of H₂O₂ can be attained.

METHODS

Catalyst Preparation and Characterization

The RQ-Ni catalyst was prepared in the following procedure. A mixture containing about equal weights of metallic Ni and metallic Al was melted at 1573 K in an argon atmosphere. Then an alloy ribbon with a cross section of approximately 0.02 × 5 mm² was prepared by a single-roller melt-spinning method. The brittle ribbon was ground to 200 mesh and added slowly to a 5 M NaOH solution at 363 K with vigorous stirring. The weight ratio between the alloy and NaOH was 1/2. The reaction system was stirred at 363 K for 1.0 h for further alkali leaching. The obtained powder was washed with distilled water until pH 7 and then washed with ethanol to replace the water. It was finally kept in ethanol for characterization and the activity test. The Raney Ni catalyst was prepared by alkali leaching of a commercially available crystalline Ni–Al alloy (Ni/Al, 50/50, w/w) using a similar procedure. As the RQ-Ni catalyst is pyrophoric, just like Raney Ni, both catalysts were weighed in a graduated tube with the protection of ethanol before the activity test.

The bulk compositions of the as-prepared catalysts were obtained by inductively coupled plasma (ICP) analysis. The BET surface area and the pore volume were determined by N₂ adsorption at 77 K on a Micromeritics TriStar 3000 adsorption apparatus. The active surface area was measured by H₂ chemisorption, assuming H/Ni(s) = 1 and a surface area of 6.5 × 10⁻²⁰ m² per Ni atom (6). Turnover frequency (TOF) was expressed as the number of H₂ molecules consumed per surface active nickel atom per second at the beginning of the reaction. The morphologies were studied by scanning electron microscopy (SEM, Philips XL 30). The X-ray diffraction (XRD) profiles were collected on a Bruker AXS D8 Advance X-ray Diffractometer with CuK α radiation. Differential scanning calorimetry (DSC, Perkin–Elmer DTA-7) was carried out under nitrogen



SCHEME 1

(99.9995%) atmosphere with a heating rate of 10 K/s. The surface composition and electronic state were detected by X-ray photoelectron spectroscopy (XPS, Perkin-Elmer PHI 5000C). All binding energy (BE) values were referenced to that of contaminant carbon ($C_{1s} = 284.6$ eV).

Reaction and Analytical Procedures

The activity test was carried out in a stainless steel autoclave (volume 220 ml) with a magnetic stirrer. A mixture of trioctylphosphate and trimethylbenzene (volume ratio 3/7) was used as the solvent, and the concentration of eAQ in the working solution was 50 g/L. The reaction conditions were as follows: 1.0 g of catalyst, 70 ml of working solution, H₂ pressure of 3 atm, and reaction temperature of 323 K. Our preliminary study revealed that the mass transfer limit can be readily eliminated by a stirring rate of 1000 rpm. The reaction process was monitored by sampling the reaction mixture at intervals, followed by O₂ oxidation. The H₂O₂ produced was extracted from the solution and then titrated by KMnO₄. As previously defined (7), the percent yield X of H₂O₂ is expressed as the ratio of the number of H₂O₂ moles to the initial number of eAQ moles in the reactor: $X = n_{\text{H}_2\text{O}_2}^t / n_{\text{eAQ}}^0 \times 100\%$, which also represents the selectivity to “active quinones.” The organic layer after H₂O₂ extraction was analyzed by high-performance liquid chromatography (HPLC) with an accuracy of 5%. eAQ

and H₄eAQ can be readily quantified by HPLC (HP 1100) with an ultraviolet detector employing the Zorbax column (ODS, 4.6 mm × 15 cm). The Finnigan Voyagen GC-MS with an HP-5 capillary column (30 m × 25 mm, 0.25 μm) was used to qualify the degradation products. It is found that H₈eAQH₂ was the main side product under the present experimental conditions.

RESULTS AND DISCUSSION

In Table 1, it can be seen that although both samples have similar bulk composition, RQ-Ni exhibits a surface area, porosity, and pore diameter higher than those of Raney Ni. It is also noted that no surface enrichment of either element occurred for the RQ-Ni catalyst by XPS analysis. SEM revealed that, compared to the typical bulky morphology of Raney Ni (Fig. 1b), the particles in RQ-Ni are smaller and the size distribution is relatively homogeneous (Fig. 1a).

XRD profiles illustrate that besides the features at $2\theta = 45.2^\circ$, 65.8° , and 83.2° , corresponding to the residual Ni₂Al₃ phase after alkali leaching (8), a broad peak centered at $2\theta = 45^\circ$ was identified for RQ-Ni (Fig. 2a), suggesting the amorphous character of the catalyst (9). When the as-prepared sample was heated to elevated temperatures in a N₂ (99.9995%) atmosphere, the diffraction lines characteristic of crystalline Ni developed at the expense of the broad peak (Fig. 2b), which is identical to that of Raney Ni with diffraction peaks at 44.0° , 51.4° , and 76.0° (Fig. 2c). DSC further revealed that the RQ-Ni sample was thermodynamically metastable, undergoing an exothermic crystallization at around 450.3 K. On the other hand, XPS showed that in both catalysts Ni and Al were predominantly in their elemental states with BEs of Ni_{2p_{3/2}} and Al_{2p} at 853.0 and 72.8 eV, respectively (10), indicating the identical electronic structure of RQ-Ni and Raney Ni.

Figure 3a exhibits the percent yield of H₂O₂ averaged in three separate runs as a function of time using both catalysts. It can be observed that over the RQ-Ni catalyst the yield of H₂O₂ increased first and then leveled off with X remaining at approximately 97%, while over Raney Ni, the yield of H₂O₂ reached a maximum of only 67% and dropped after prolonged reaction time. These

TABLE 1

Some Characteristics of the RQ-Ni and Raney Ni Catalysts

Catalyst	Bulk comp. (molar ratio)	Surf. comp. ^a (molar ratio)	S _{BET} (m ² /g)	V _{pore} (cm ³ /g)	d _{pore} (nm)	S _H (m ² /g)	TOF (s ⁻¹)
RQ-Ni	Ni _{69.6} Al _{30.4}	Ni _{69.3} Al _{30.7}	111.2	0.10	3.69	27.3	0.56
Raney Ni	Ni _{68.0} Al _{32.0}	—	98.3	0.073	3.21	43.0	0.60

^a The surface composition was obtained by fitting the Ni_{2p_{3/2}} and the well-resolved Al_{2s} peaks with the Gaussian-Lorentzian lineshape after subtracting a linear background.

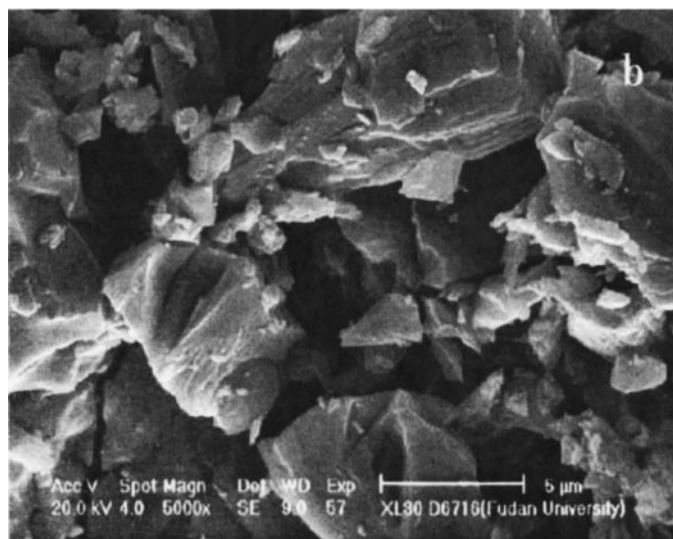
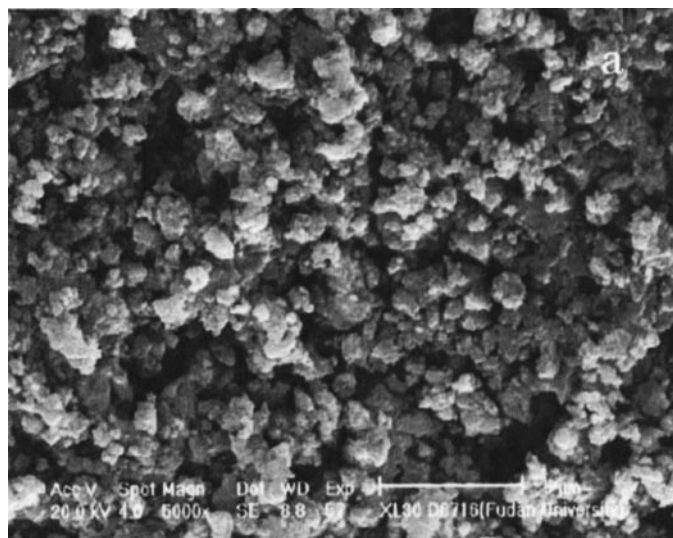


FIG. 1. SEM morphology of the (a) RQ-Ni and (b) Raney Ni samples.

results clearly demonstrate a selectivity of RQ-Ni prepared from the rapidly quenched Ni-Al alloy in the hydrogenation of eAQ to “active quinones” higher than that of Raney Ni derived from the conventional Ni-Al alloy.

In order to get an insight into the discrepancies in the selectivity between these two catalysts, the evolutions of eAQ and H₄eAQ were monitored and plotted in Fig. 3b. It should be stressed that eAQ in Fig. 3b virtually denotes the summation of unreacted eAQ and eAQ hydrogenated to eAQH₂, while H₄eAQ is equal to H₄eAQH₂ in quantity, as demonstrated by the reduction–oxidation cycle shown in Scheme 1. On RQ-Ni, H₄eAQ did not appear in the first 20 min, indicative of the high selectivity to eAQH₂, while on Raney Ni, H₄eAQ was produced as soon as the hydrogenation commenced. Also according to GC-MS, H₈eAQH₂ was

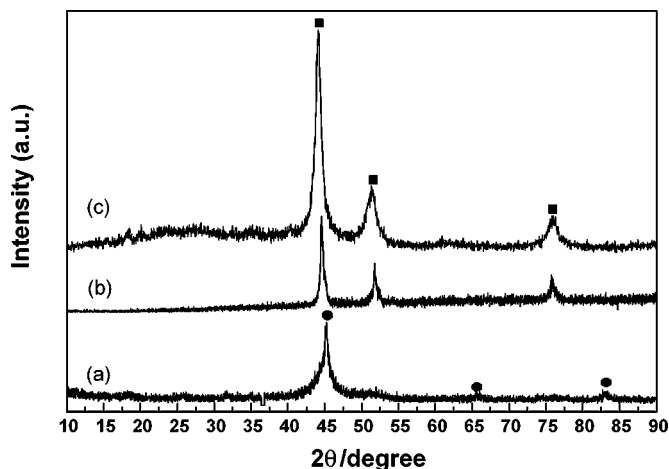


FIG. 2. XRD profiles of (a) the as-prepared RQ-Ni, (b) RQ-Ni annealed at 903 K in a high-purity N₂ atmosphere, and (c) Raney Ni. ●, Ni₂Al₃; ■, Crystalline Ni.

also produced immediately on Raney Ni. So it can be readily concluded that the RQ-Ni catalyst prepared from the rapidly quenched Ni-Al alloy exhibits a selectivity higher than that of Raney Ni in carbonyl group hydrogenation

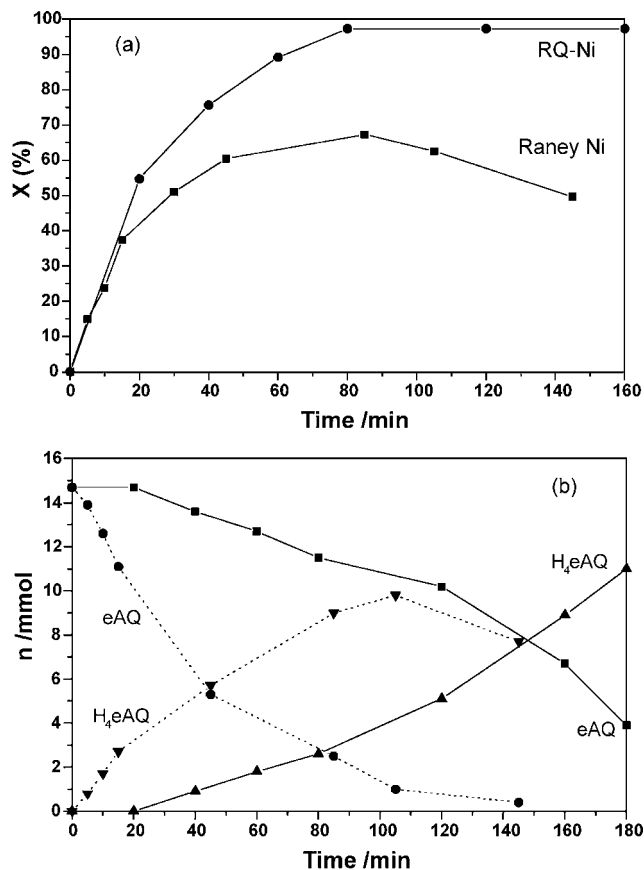


FIG. 3. (a) The percent yield X of H₂O₂, and (b) the evolution of eAQ and H₄eAQ over the RQ-Ni (—) and Raney Ni (···) catalysts as a function of reaction time. The reaction conditions are listed in the text.

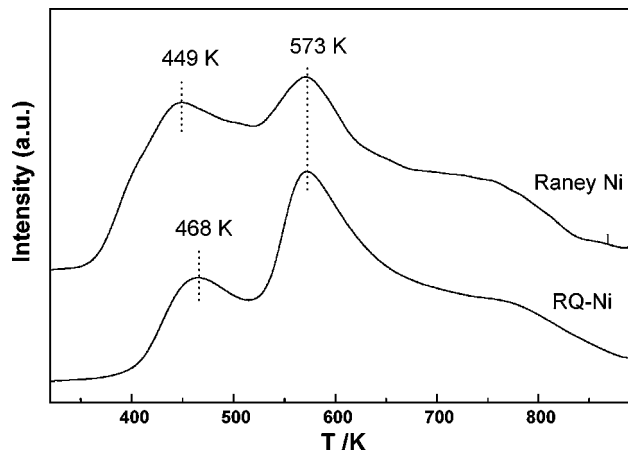


FIG. 4. The H_2 TPD features over the RQ-Ni and Raney Ni catalysts.

where an aromatic ring coexists, thus leading to a higher yield of H_2O_2 and a lower consumption of H_2 and expensive eAQ, which is highly preferred in the industrial process.

As ICP and XPS did not give substantial difference in the chemical composition and electronic states between RQ-Ni and Raney Ni, their different catalytic behavior in eAQ hydrogenation may be ascribed to the structural effect. Mikhailenko *et al.* found that the relative amount of the weakly and strongly bound hydrogen determines the selectivity of eAQ hydrogenation on pure and oxide-modified Raney Ni (11), since the weakly bound hydrogen is highly reactive in aromatic ring hydrogenation (12). Because the pristine alloy was prepared by the rapid quenching technique, it is expected that the RQ-Ni sample is highly defective as also implied by XRD and DSC. Due to the coordinatively unsaturated nature, the defects tend to bond tightly with hydrogen, which is well corroborated by H_2 TPD spectra. Figure 4 unambiguously shows that the population of the strongly bound hydrogen is much higher than that of the weakly bound hydrogen on RQ-Ni, while on Raney Ni the population of these two species is comparable. On the other hand, according to Table 1, we noted that the active surface area (S_H) is larger on Raney Ni. Referring to the dual-site mechanism, which suggests that the hydrogenation of the aromatic ring involves eAQH₂ and two hydrogen atoms bonded on two adjacent metal atoms (13), it is proposed that the higher the concentration of hydrogen on the cata-

lyst surface, the higher the possibility for aromatic ring hydrogenation. A detailed mechanistic study is needed to fully elucidate the superior selectivity of the RQ-Ni catalyst prepared from the rapidly quenched precursor for eAQ hydrogenation.

CONCLUSIONS

The skeletal Ni catalyst derived from the rapidly quenched Ni–Al alloy gave a yield of hydrogen peroxide in eAQ hydrogenation higher than that of Raney Ni. Its superior selectivity is ascribed to the preferential population of strongly bonded hydrogen on its defective surface.

ACKNOWLEDGMENTS

This work is supported by the Major State Basic Research Development Program (Grant G2000048009) and the National Natural Science Foundation of China (20073008).

REFERENCES

1. Ulmann, T., "Encyclopedia of Industrial Chemistry," Vol. A3, p. 443. VCH, Weinheim, 1989.
2. Kroschwitz, J. I., and Howe-Grant, M., "Kirk-Othmer Encyclopedia of Chemical Technology," 4th ed., Vol. 13, p. 961. Wiley, New York, 1995.
3. FMC Corp., Hydrocarbon Process. Petrol Refiner **11**, 184 (1963).
4. Cronan, C. S., *Chem. Eng.* **6**, 118 (1959).
5. Drelinkiewicz, A., Hasik, M., and Kloc, M., *Catal. Lett.* **64**, 41 (2000).
6. Bartholomew, C. H., and Pannell, R. B., *J. Catal.* **65**, 390 (1980).
7. Drelinkiewicz, A., Hasik, M., and Kloc, M., *J. Catal.* **186**, 123 (1999).
8. "PDFMaint Version 3.0, Powder Diffraction Database," Bruker Analytical X-ray Systems GmbH, 1997.
9. Wontergem, J., Mørup, S., Charles, S. W., and Wells, S., *Nature* **322**, 622 (1986).
10. "Handbook of X-ray Photoelectron Spectroscopy," Perkin-Elmer Corporation, 1992.
11. Mikhailenko, S. D., Fasman, A. B., Maksimova, N. A., and Leongard, E. V., *Appl. Catal.* **12**, 141 (1984).
12. Roberts, J. D., and Caserio, M. C., "Basic Principles of Organic Chemistry," W. A. Benjamin, Elmsford, NY, 1964.
13. Santacesaria, E., Di Serio, M., Velotti, R., and Leone, U., *J. Mol. Catal.* **94**, 37 (1994).